Available online at www.sciencedirect.com
ScienceDirect
Journal of the European Ceramic Society 27 (2007) 115–123
www.elsevier.com/locate/jeurceramsoc

Precursors for the combustion synthesis of metal oxides from the sol–gel processing of metal complexes

Mauro Epifani [a,*], Enrico Melissano [a], Giovanni Pace [a], Monica Schioppa [b]

[a] *Consiglio Nazionale delle Ricerche, Istituto per la Microelettronica ed i Microsistemi, CNR-IMM, via Monteroni, 73100 Lecce, Italy*
[b] *ENEA C.R. Brindisi, UTS MAT, S.S.7, km 7+300, 72100 Brindisi, Italy*

Received 28 January 2006; received in revised form 13 April 2006; accepted 14 April 2006
Available online 5 June 2006

Abstract

Sol–gel processing of methanol solutions of Cu(II) acetylacetonates was used for obtaining controlled polymerization of the complex molecules. The resulting sols were evaporated and the resulting precipitate was heated until a self-sustaining combustion reaction took place. The simultaneous presence of nitrate ions and the acetylacetonato ligands resulted in a sharp combustion process, characterized by low activation temperature and intense exothermic feature. The same processing was applied to other metals and other ligands, showing that the sol–gel processing of transition metal complexes can be a simple, convenient, flexible generalization of the citrate–nitrate method for preparing precursors for the combustion synthesis of oxide powders. Moreover, the controlled sol–gel processing of the metal complex can be used as a tool for controlling the precursor structure and, hence, the morphology of the final product.

Keywords: Combustion synthesis; Powders-chemical preparation; Sol–gel processes; Transition metal oxides

1. Introduction

Combustion synthesis[1] is becoming one of the most popular methods for the preparation of a wide variety of materials, ranging from non-oxides, such as borides, nitrides, carbides, etc., to simple and complex oxides. The diffusion of the technique, which, depending on the experimental conditions, is described as solution combustion synthesis (SCS), gel-combustion synthesis, sol–gel combustion, etc., is due to the simplicity, the broad applicability range, the self-purifying feature due to the high temperatures involved, the possibility of obtaining products in the desired size and shape. The SCS method is rapidly emerging as one of the most-convenient methods for the preparation of oxide materials. An aqueous solution of a redox system constituted by the nitrate ions of the metal precursor, acting as oxidizer, and a fuel like urea, glycine, citric acid (citrate or Pechini method[2]) or many others[1c,3] is heated up to moderate temperatures and, upon dehydration, the strongly exothermic redox reaction develops, which is generally self-sustaining and provides the energy for the formation of the oxide. Oxide materials produced with this method include several ferrites[4] and spinels,[5] tin oxide[6] and antimony tin oxide (ATO),[7] ceria,[8] ferroelectric materials,[9] iron oxide,[10] zinc oxide,[11] protonic conductors[12] and various solid solutions.[13] Many alternative procedures have been recently proposed, based on the exploitation of different fuels with well defined advantages and properties,[1c] on the use of metal precursors already containing the organic fuel in their molecule,[1c] and on solventless procedures using the dry mixing of the metal nitrates and the fuels.[14] A sol–gel variation of the citrate method has been proposed, based on the study of the influence on the combustion characteristics of pH adjustments in the starting solution.[4b,13a,15] Actually, in the citrate method[2] a viscous gel is already obtained during the heating of the starting solution. The addition of ammonia for adjusting the pH may result in further networking of the precursor molecules, by forced hydrolysis, so justifying the classification as sol–gel combustion method. In a previous work,[16] we have used the sol–gel processing of indium complexes for depositing high quality In_2O_3 thin films, and we have observed a strong exothermic phenomenon during the heating of the corresponding dried precursor. This result suggested a possible generalization of the citrate method by using different ligands to complex the

* Corresponding author. Tel.: +39 0831 508544; fax: +39 0831 519106.
E-mail address: mauro.epifani@le.imm.cnr.it (M. Epifani).

0955-2219/$ – see front matter © 2006 Elsevier Ltd. All rights reserved.
doi:10.1016/j.jeurceramsoc.2006.04.084

metal ion. Actually, complexation by other ligands has been commonly reported, when using such fuels as urea, amines or citric acid. But with these fuels molecular precursors anyway are formed in solution, while we were interested in a generalization of the polymeric gel formed upon heating of the solutions containing citrates. This result can be achieved by polymerization of the complex molecules through their sol–gel processing. As stated before, ammonia addition to citrate–nitrate solutions has been reported for pH adjustment, resulting in a sort of sol–gel processing. In this work, we show that the citrate method can be seen as a particular case of a general procedure based on metal complexation by a ligand, followed by sol–gel processing by ammonia. The role of ammonia, and in general of bases, will be shown as explicitly directed to the controlled inorganic polymerization of the metal complexes. In this way a general method is introduced for obtaining non-molecular precursors through of a hybrid process where the precursors are prepared in solution and then extracted by evaporation before the combustion step. An immediate advantage of these precursors is that the combustion process requires low activation temperatures and proceeds through highly exothermic processes, showing the possibility of obtaining pure powders without any post heat-treatment. Moreover, the tuning of the precursor molecular structure through its processing introduces the possibility of controlling the morphology and the structure of the final product. As a case study, we choose the synthesis of CuO powders, for the possibility of having simple and deeply studied Cu^{2+} complexes that are readily identified by optical absorption spectroscopy. The occurrence of similar combustion processes in analogous precursors of other oxides will be shown for completeness.

2. Experimental

The starting solutions were prepared by dissolving 2 g of $Cu(NO_3)_2{\cdot}2.5H_2O$ in 10 ml of methanol, followed by the addition of acetylacetone (acacH), and the initially blue solutions became deep-green colored. An ammonia solution (30 wt% solution in water) was then added, eventually followed by the addition of concentrated nitric acid (65 wt% solution in water) for dissolving any eventual precipitate. The various acacH:Cu, NH_3:Cu and H^+:Cu molar ratios employed will be denoted with R_L, R_B and R_H, respectively. After stirring for 24 h, the solutions were concentrated into a rotary evaporator (bath temperature 35 °C, final pressure 7500 Pa), until a green precipitate remained. The precipitate was collected and inserted into a high beaker heated onto a hot plate. During heating up to 150–170 °C, a flame spontaneously developed from the precipitate and propagated to the regions of the precipitate that had not been ignited yet. After a few seconds, a black powder remained, which in the following will be denoted as post-precursor. It was collected and heat-treated at 500 °C in a tubular oven The choice of CuO as a case study resulted in some additional problematic, due to the simultaneous presence of various Cu oxides and even of Cu, after the combustion stage. For this reason the heat-treatments of the post-precursor were carried out in oxygen atmosphere, but it must be remarked that this is required by the peculiar behavior of the Cu precursor. For other oxides, a heat-treatment in air can be sufficient for purifying the various post-precursors. For comparison, other precursors were prepared by substituting Cu with Zn, Fe or In or substituting acacH with diethylenetriamine (dien), trioctylphosphine (TOP) or hexanethiol (HA).

UV–vis optical absorption spectra on the starting solutions were obtained on a Perkin Elmer (model Lambda 19) spectrometer. FTIR measurements on the starting solutions or on the dried or heat-treated products were carried out by a Nicolet spectrometer. The solution samples were prepared by placing a drop of the solution on a KBr pellet and then evaporating the solvent at room temperature. X-ray diffraction (XRD) patterns on the powders were recorded in the 10–80° range with a Philips, PW 1880 diffractometer, using the Kα radiation emitted by a Cu target. Simultaneous differential thermal analysis/thermogravimetric (DTA–TG) measurements on the dried precursors were carried out with a Netzsch-STA 429 Simultaneous Thermal Analyzer at a scan rate of 10 °C min^{-1}. The measurements were conducted in a dynamic atmosphere of air using a flow rate of approximately 100 ml min^{-1} in a temperature range from 25 to 500 °C by placing about 10 mg of sample into platinum crucibles. The powder morphology was observed with a Jeol JSM6500F Field Emission Scanning Electron Microscope (FE-SEM).

3. Results and discussion

When a suitable ligand is introduced into a metal ion solution, the following addition of a base results in different phenomena with respect to a solution where no ligand is present. When no ligand is present, the base addition usually results in precipitation of the hydrated, amorphous oxide. This occurs since the solvent molecules are usually weaker ligands than the OH ions generated by the base addition, and fast and extensive hydrolysis of the metal ion takes place, together with inorganic polymerization resulting in the formation of large, insoluble oxide species. The different result of base addition when a stronger ligand is present is due to the harder displacement of the ligand from the metal coordination sphere, so preventing or delaying the hydrolysis of the metal ion. Of course, this result depends on the strength of the ligand-ion bond. Thus, it can be expected that a whole range of structures will be generated by tuning the base and ligand concentrations. In particular, the addition of the base will result in a different extent and pathway of the inorganic polymerization, depending on the ligand structure and concentration, and the final result could resemble a range of complex, non-molecular species. Finally, the water concentration will obviously influence the extent of the sol–gel reaction of the precursor, but the water:metal molar ratio is implicitly fixed by the initial hydration of the metal salt and by the base and acid concentrations. Further water can be added in order to modify the extent of the sol–gel reaction, but we did not consider this aspect in detail.

We have observed that upon solvent extraction, a precipitate is obtained that can be readily redispersed when the solvent is again added, so showing that hydrolysis and cross-linking reactions do not extend throughout the precursor to form an actual gel, and that the sol-to-gel transition is at most localized in the smaller regions constituted by the particles in the sol. In some cases, a precipitate was obtained upon base addition, even

in the presence of the ligand, provided sufficient base excess was used. The precipitate was then re-dissolved by addition of nitric acid. Thus, the amount of acid may constitute a further variable determining the final structure of the particles in the sol. We initially concentrated on simple acetylacetonato ligands, since they bond to the metal ions through their oxygen atoms and cannot pollute the final product as it could happen when using thio or phosphine complexes, for instance. Amines were not considered since they may act as strong bases so interfering with the following base addition. These last ligands were tested in a subsequent part of the work.

The actual determination of the structure and of the composition of the sol species would be an extremely complex task, but general indications about the actual influence of the various additives on the sol structure could be obtained by optical measurements on the as-obtained sols. In Fig. 1 the results are shown concerning solutions with different synthetic parameters. While the general structure in this wavelength range is constituted by two peaks centered at about 250 and 280 nm, which are typical of Cu diketonato complexes,[17] it is remarkable that the peak width, the position and the relative intensities depend on the processing parameters. In particular, a continuous blue-shift of the peak is evident in panels A and B of the figure with increasing the R_H and R_B and the R_H and R_L values, respectively. These results are indicative of a change of the metal ion symmetry and of the ligand strength and, hence, of the presence of different structures in the sols. Further indications come from the analysis of the FTIR spectra, shown in Fig. 2, measured on both dried samples and starting solutions.

First of all, we will note that the sols are highly reactive to atmospheric exposure, so the analysis on the solutions is not completely indicative of the bonds actually presents in the sols and the typical bands of acetylacetonato complexes are not clearly seen in the spectra C–E. What is clearly observed and of interest for the present discussion is the presence of two peaks at about 1390 and 825 cm^{-1}. The band at 1390 cm^{-1}, in particular, strongly depends on the sol processing parameters, as concerns the shape and the peak position. The band at 825 cm^{-1} is due to the nitrate ion out-of-plane deformation[18] and is unchanged by the processing conditions, while a strong and sharp band for the asymmetric stretching of the nitrate ion is expected at 1385 cm^{-1}.[18] Moreover, the NH_3 symmetric deformation band for metal ammine complexes is reported in the 1370–1000 cm^{-1} range.[19] So, we conclude that the band at about 1390 cm^{-1} is due to the overlapping of the nitrate and of the metal–ammine complex bands. Thus, its shape and position changes according to the processing conditions directly reflect a varying local symmetry at the metal ion sites in the precursors, again showing that different base, ligand and acid ratios result in different structures in the sol. In particular, in curve A the sharp peak typical of the nitrate only is observed at 1385 cm^{-1}, as expected from a precursor prepared without ligand and acid, and in which most of the solvent has evaporated during the drying process. The presence of the metal–ammine complex is further demonstrated by the asymmetric NH_3 stretching band at about 3200 cm^{-1}, whose intensity is closely related with the base concentration in the corresponding sol (see Electronic Annex 1 in the online version of this article). A final, fundamental detail concerns the low fre-

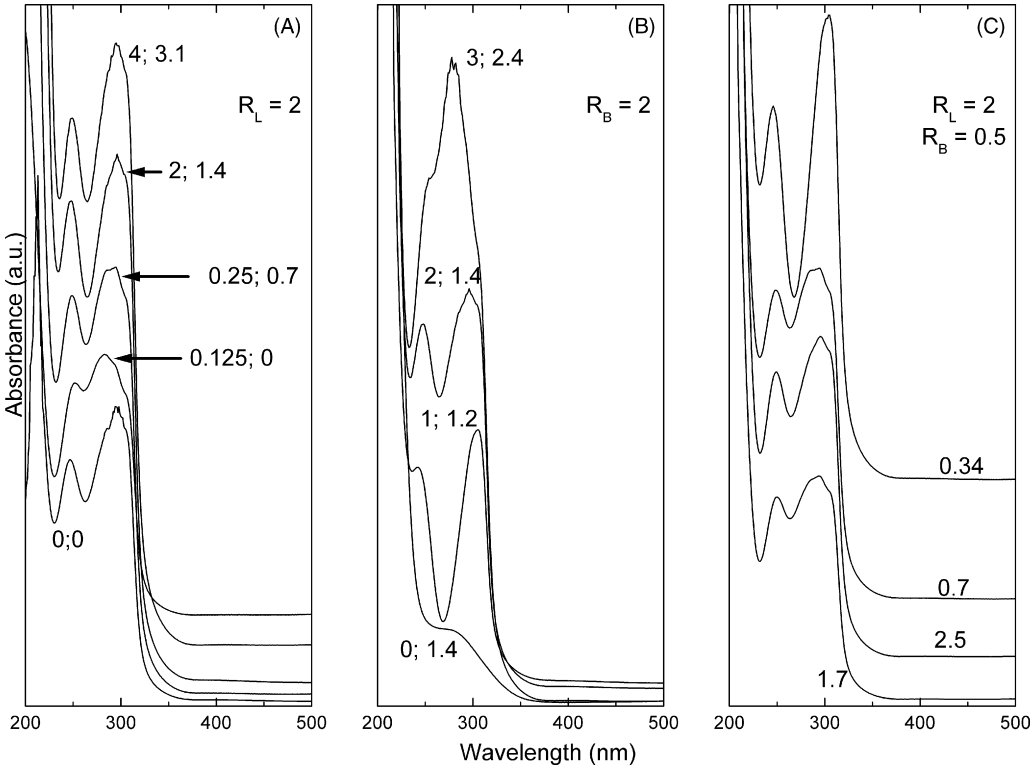

Fig. 1. UV–vis absorption spectra measured on (A) solutions with $R_L = 2$ and the indicated R_B and R_H values, (B) solutions with $R_B = 2$ and the indicated R_L and R_H values, and (C) on solutions with fixed R_L and R_B and the indicated R_A values. The curves have been vertically displaced for clarity.

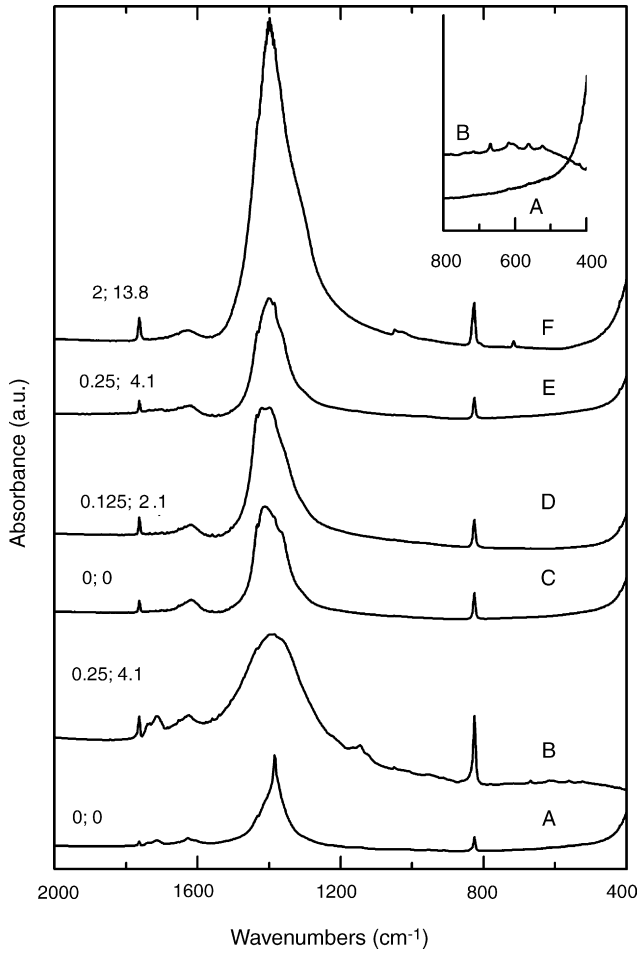

Fig. 2. FTIR spectra measured on dried precursors (A and B) and starting solutions (C–F) prepared with $R_L = 2$ and the indicated R_B and R_H values.

quency region of the IR curves. While the curves generally show an increasing absorbance below 800 cm^{-1}, in curve B a broad band is observed in that region, which is magnified in the inset in Fig. 2, where the comparison with curve A is shown. An absorption band in that region is characteristic of metal oxides,[18] while the broadening is indicative of amorphous species. Since curves A and B refer to the same precursor in different conditions, we conclude that upon the drying process condensation of the sol species takes place, giving rise to polynuclear Cu-containing species. It is clear at this point the explicit role of ammonia in determining a sol–gel processing of the metal nitrate and in obtaining non-molecular species, whose structure can be tuned by varying the processing parameters. We only note that, as previously mentioned, the precipitate can be easily redissolved in methanol or water, indicating that the polycondensation process is limited and can produce only small aggregates.

The chemical difference between the various precursors determined a marked difference in the thermal behavior, as clearly evidenced by the thermal analyses carried out on the dried samples, whose results are summarized in Fig. 3. We first note that a careful calculation of the energy involved in the various processes was made unreliable by the possibility of different degrees of drying of the precursors, implying possible compositional differences. In panel 1 the DTA and TG curves related to the copper nitrate dissolved in methanol and recrystallized are shown. This procedure was used in order to reproduce as much as possible the same experimental conditions for all the analyzed precursors. Only intense and broad endothermic phenomena are observed in the DTA trace until a temperature of 300 °C is reached, where the mass loss stops and no other peaks are observed. Since the curves are very similar to those for the pure nitrate (see Electronic Annex 1 in the online version of this article), the dissolution in methanol and the following drying only add some methanol ligands that are desorbed during heating together with the hydration water, followed by the decomposition of the nitrate ion at higher temperatures. In panel 2 the DTA and TG traces are shown for the dried precursor obtained with basic precipitation of the nitrate solution, and that should hence contain copper hydroxide species. An intense exothermic peak is observed at about 270 °C, simultaneously with a large mass loss. This result is expected and is due to the combustion of ammonia triggered by the nitrate ions. For confirming this interpretation, we prepared an analogous precursor by substituting the Cu nitrate with the chloride, and the corresponding DTA trace is shown in curve A of the inset in panel 1. The difference with panel 2 clearly shows the importance of nitrate ions in triggering the combustion reaction. The next step was the analysis of a precursor prepared with acetylacetone without any base addition, with the results shown in panel 3. A sharp exothermic peak is observed at about 147 °C, followed by other less intense peaks at slightly higher temperatures and by another intense peak at about 450 °C. This result could be interpreted by combustion of the copper acetylacetonato complex, analogously to the combustion observed in panel 2. The peak at about 450 °C would then be the oxidation of the various carbonaceous residuals. Since it was in doubt whether the first exothermic peak at 147 °C was triggered by the nitrate ions, an analogous precursor was prepared by substituting the copper nitrate with the chloride. The corresponding DTA trace is shown in the inset in panel 1 (curve B), and an exothermic peak is observed, even though it occurs at about 350 °C and is very broad. So the complex itself is subjected to an exothermic decomposition, but the presence of the nitrate ions makes the process much more fast and efficient, with a much lower activation temperature. Finally, a precursor was prepared by the whole sol–gel processing, and the DTA/TG traces are shown in panel 4. This time an extremely intense peak is observed at a lower temperature than in panel 3, with a much narrower development of the combustion. Moreover, the process is extremely efficient in eliminating any organic residual, and only very weak exothermic peaks are present below 400 °C. From the comparison with the previous results, it appears that the combustion of the acetylacetonato complex triggered by the nitrate ions in turns activates the combustion of ammonia ligands which, as shown in panel 2, is itself very exothermic and, as a whole, the intense combustion shown in panel 4 is generated. About the mechanisms involved in the combustion process, some preliminary observations can be presented. First of all, when drying a sol at higher bath temperatures (70 °C), sudden formation of vapors occurred in the rotating flask when the precursor was in advanced state of drying. The product was almost completely constituted by metallic copper.

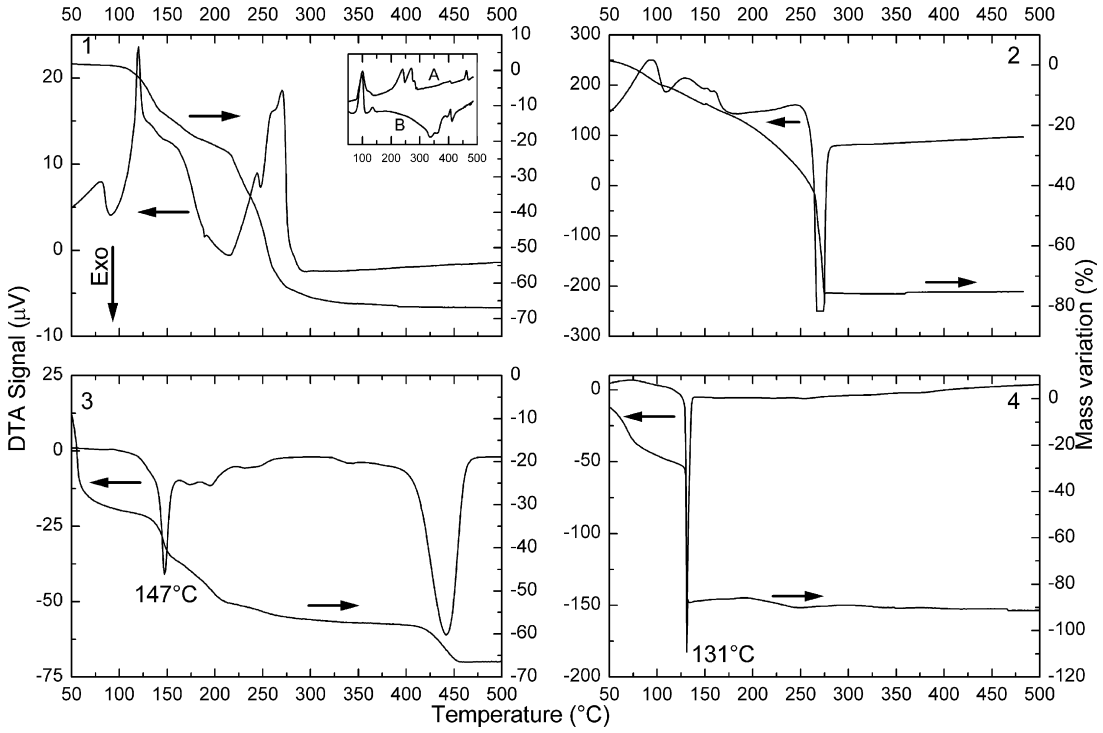

Fig. 3. DTA/TG traces measured on dried precursors prepared by nitrate dissolution/recrystallization (panel 1), or by solution processing with $R_L = 0$, $R_B = 2$ and $R_H = 1.4$ for panel 2, $R_L = 2$, $R_B = 0$ and $R_H = 0$ for panel 3 and $R_L = 2$, $R_B = 0.25$ and $R_H = 4.1$ for panel 4.

This indicates that during the combustion step, the formation of the oxide is due to the reaction of metal ions with atmospheric oxygen, favored by the high temperature generated by the combustion, and not by a decomposition of the acetylacetonato ligand leaving its oxygen atoms bound to the metal center. This result is expected, since a direct extraction of oxygen from the acetyacetonato or other ligands occurs only in particular organic reactions[20] very different from the combustion synthesis. The second observation concerns the meaning of the term "combustion" in the present systems. Curve B in the inset in Fig. 3 shows that the decomposition of the acetylacetonato complex in the absence of the nitrate has a very high activation temperature. Keeping also into account the previous observation, we can conclude that the presence of the nitrate ion can promote the breaking of the metal–acetylacetone bond, which provides energy for the breaking of similar bonds and of the metal–ammine bond, followed by the combustion of the re-generated free ligands. The latter could then be viewed as intermediate for forming the precursor during the sol processing and drying, then becoming the fuel for the combustion process. In principle, the process could work without any additional fuel, by simply relying on the energy generated by the complex decomposition, provided the latter is sufficient for a self-sustaining process. Of course the whole process will be a complex overlapping of the various steps, not excluding the possibility of direct combustion of the ligands still bound to the metal centers. The reason for having such low activation temperatures in the presence of the nitrate is not clear, and could involve initial oxidation of free organics in the dried precursor, providing the initial energy, but, as evidenced by further experiments discussed below, direct oxidation of the metal–acetylacetone bond seems more likely. We remark again the low activation temperature of the whole process, and the possibility of obtaining a pure product without any post heat-treatment, by eventually tuning the composition of the combustion atmosphere. In panel 4 of Fig. 3, indeed, after the first exothermic peak there are almost no other obvious phenomena. This indication was reinforced by the results obtained for other metals, in a series of experiments carried out for showing the generality of the process. The results are shown in Fig. 4.

The structure of the DTA traces is very similar for the various precursors, with a very intense exothermic peak at low temperatures. This result shows the possibility of easily generalizing the

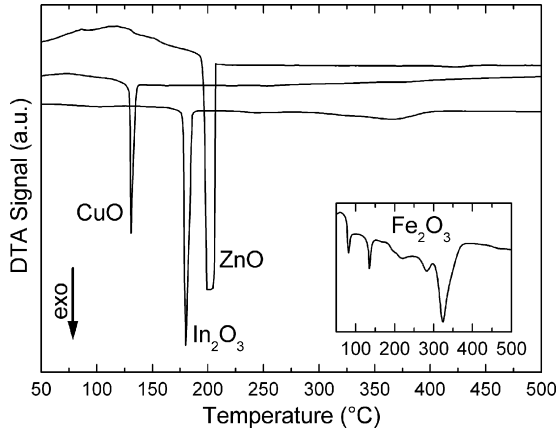

Fig. 4. DTA traces measured on the indicated dried oxide precursor. The processing parameters were $R_L = 2$, $R_B = 0.25$ and $R_H = 4.1$.

process to other oxides, but also evidences that the combustion mechanism most probably involves the initial breaking of the metal–acetylacetonato complex more than the oxidation of free organics. The exothermic peak position indeed spans a range of about 100 °C depending on the metal (the processing conditions are identical for the various sols, apart for the presence of different metal nitrates), which makes less likely the presence of a single initial reaction. It is important to observe that in the case of iron a very well dried precursor was analyzed, and in this case multiple exothermic peaks are observed with the last one at about 350 °C. A possible different structure of the precursor could be invoked, but this result can also be an indication that using not perfectly dried precursor is useful in increasing the efficiency of the process, with the residual solvent molecules that act as an additional fuel.

The possibility of generalizing the ligand was further tested, as concerns the presence of similar exothermic phenomena during the heating of the precursor. The precursors were prepared, as described in Section 2, similarly to those containing acetylacetone. We only remark that ammonia was introduced even in the preparation of these new precursors for having similar conditions. Nevertheless, in the case of dien it could be unnecessary, while in the case of TOP or hexanethiol it could result in undesired reactions with the ligands, and its use should be carefully evaluated. The results of the DTA analyses of the new precursor are shown in Fig. 5, and the presence of exothermic peaks is clear, proving that acetylacetone is not strictly needed for developing the precursor combustion. The different position of the exothermic peaks reflects the specific bonding energy of the ligands with the copper ions. In the case of dien a large amount of organic residuals are present after the first exothermic peak, since a broad and intense peak is observed at high temperatures. Whether a particular ligand should be selected will depend on specific considerations about the investigated system, but it is clear that the possibility of using different ligands remarkably extends the applicability of the process.

The phase composition and evolution of the combustion product was monitored by XRD as a function of the heat-treatment temperature. While the FTIR spectra do not show any trace

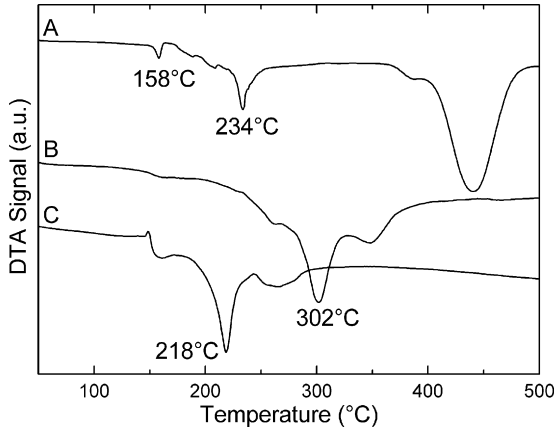

Fig. 5. DTA traces measured on precursors prepared with $R_L = 2$, $R_B = 0.25$ and $R_H = 0$, but substituting acetylacetone with (A) diethylenetriamine, (B) trioctylphosphine and (C) hexanethiol.

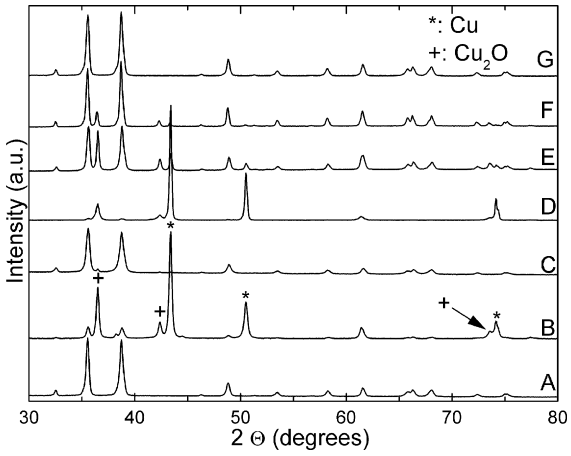

Fig. 6. XRD patterns measured on post-precursors and heat-treated powders, prepared as described in the text.

of organic residuals after the combustion step (see Electronic Annex 1 in the online version of this article), the macroscopic appearance of the sample indicated the presence of carbonaceous residuals, for whose elimination heat-treatments of the powders was required. In this step we had to face a supplementary problem, due to the formation of various Cu-containing compounds. Fig. 6 summarizes the results of the XRD studies. Pattern A concerns a powder obtained by heat-treating up to 500 °C the same precursor of panel 1 in Fig. 3. As expected, since such precursor is solvated copper nitrate, the product is pure CuO.

The result was remarkably different when the other precursors were heat-treated. Pattern B is related to a sample prepared with $R_L = 2$, $R_B = 0$ and $R_H = 0$ (same sample of panel 3 in Fig. 3) soon after the combustion step. Metallic Cu is predominant together with Cu_2O and, to a much lower extent, CuO. This result indicates that indeed the formation of the oxide can be mainly attributed to reaction with atmospheric oxygen, and most probably in our specific experiment the environment was oxygen depleted due to the occurring combustion reactions. A practical indication is the use of a flow of oxygen during the combustion process in order to prevent substoichiometric oxygen concentrations. After heat-treating the combustion product at 500 °C, pure CuO was obtained, with only a small trace of Cu_2O (pattern C). The combustion of the sol–gel processed precursor ($R_L = 2$, $R_B = 0.25$ and $R_H = 4.1$, like panel 4 of Fig. 3) again resulted in a phase mixture but with a much larger prevalence of Cu and the almost total absence of CuO (pattern D). After heat-treating at 500 °C in oxygen flow (pattern E) the Cu phase was partially converted to CuO and Cu_2O, with a further enhanced conversion of Cu and Cu_2O to CuO after heat-treatment at 650 °C (pattern F). Instead of heat-treating at even higher temperatures, we observed that in the case of the acetylacetonato precursor (pattern B), a single phase was obtained after heating at 500 °C and that after the combustion a certain fraction of CuO was present. By comparison with patterns D–F, we concluded that CuO could act as a seed for the conversion of the other phases to CuO at lower temperatures. So the post-precursor of pattern D was heat-treated up to only 500 °C in flowing oxygen after mixing with 3 mg of the pure CuO powder of pattern A, and indeed

a complete conversion to CuO was obtained, as shown in pattern G. Apart for these peculiarities of the CuO system, the most interesting feature is the difference of the phase composition of the two post-precursors (patterns B and D) indicating the presence of more enhanced reducing conditions in the combustion of the sol–gel processed precursor. The reason is not clear, but could be related to the extended organics oxidation activated by the highly exothermic phenomena developed in the combustion (see Fig. 3), requiring more complete oxygen depletion from the surrounding atmosphere.

Generalizing the sol–gel citrate process may result in several practical advantages, since a field is open in principle for reaching low combustion activation temperatures, complete organics elimination without post heat-treatments and, eventually, unusual or metastable phases resulting from the composition of the starting precursor. Another interesting perspective is the control of the product morphology through the variation of the precursor processing. As evidenced in the previous paragraphs, different activation temperatures, organics elimination pathways and reaction enthalpies are associated with the various precursors, which could act on the nucleation, dissolution and re-precipitation rates of the oxide grains. Direct observations of selected samples gave further support to this assumption. The results are shown in Fig. 7. FE-SEM observations were preferred to TEM observations of the aggregated powders, that did not allow a clear observations of the morphological features.

In general, in all the images a lamellar morphology can be discerned, but while in sample A, corresponding to pattern A in Fig. 6, the lamellae are very clearly visible, the morphology of sample B (pattern G in Fig. 6) is characterized by regions constituted by smaller, less regular lamellae. Finally, the acetylacetonato-derived powders in sample C (pattern C in Fig. 6) are characterized by structures that can resemble overlapped lamellae, but have a finely granular appearance. Apart for the specific consequences of the seeding technique used for preparing pure CuO in the case of the sol–gel processed precursor, it finally appears that the specific precursor processing has a remarkable influence on the final powder morphology. The details of such dependence are not clear, and it is not immediate to state a direct influence of the different exothermic phenomena involved. In general, however, the obtained powders seem to share a common feature of the materials prepared by the combustion techniques, consisting in a morphology that is anyway dictated by the sharp and intense exothermic phenomena involved. From this point of view, it is important to remark an experimental observation carried out during the sol preparation stage. If the solvent is slowly evaporated, crystals of the precursor appear on the bottom of the container. The crystal growth is directly dictated by the structure of the precursor species in the solution, so the differences in the sol processing will be enhanced and kept until the combustion step, differently from the evaporation procedure, yielding a compressed precipitate. While the principle seems promising, the first attempts show that the occurrence of the exothermic combustion is anyway predominant in determining the product morphology, indicating that the exploitation of precursor crystals for controlling the product morphology still requires remarkable efforts.

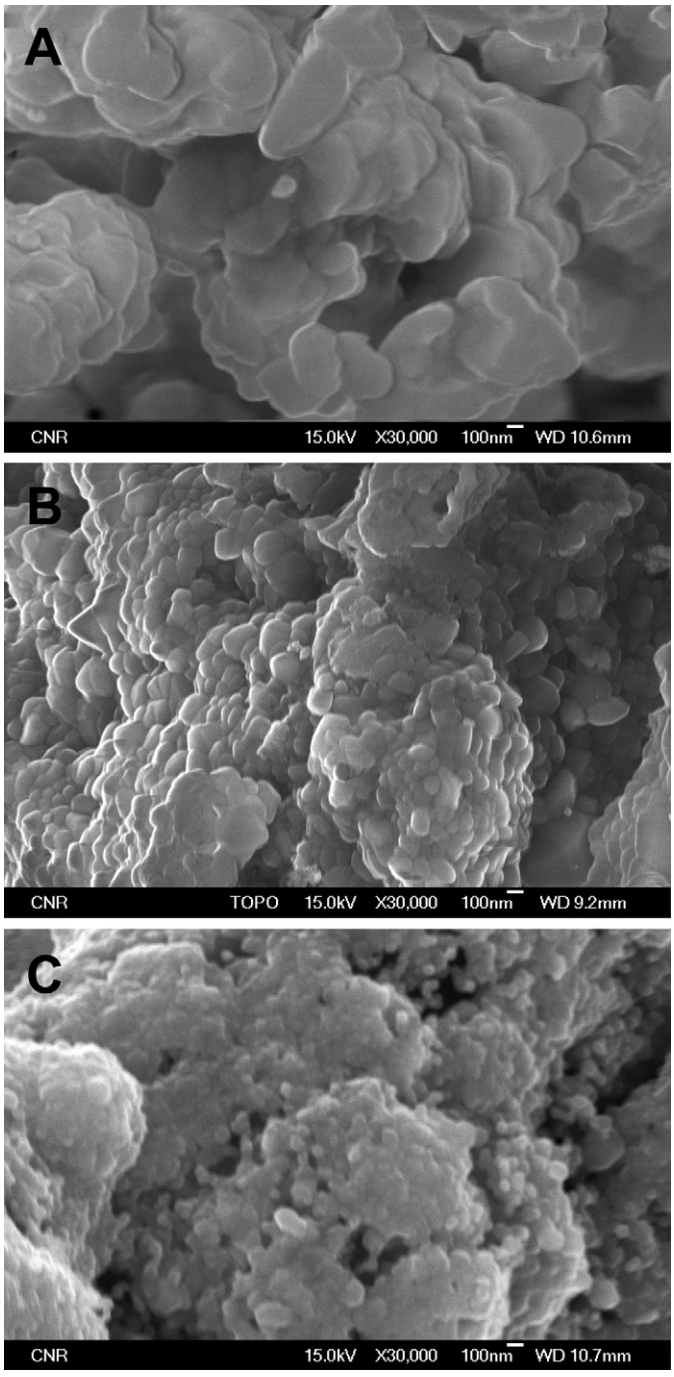

Fig. 7. FE-SEM images of the same powders of (A) pattern A, (B) pattern G and (C) pattern C in Fig. 6.

The use of methanol as the solvent could introduce toxicity concerns. It was used in our process since it allows the dissolution of a larger number of metal salts if compared to ethanol, so allowing an immediate application of the process to many different systems, without any need for finding different solvents, which could influence the initial sol preparation. Of course, toxicity concerns related to methanol could be overcome by using ethanol after verifying that the latter is a suitable solvent and does not modify substantially the sol preparation. Finally, the precursor crystal growth by freeze-drying techniques could allow an

easier recycling of the solvent, improving the economic features of the process. While this is a technological concern, another fundamental topic is the extension of the process to multicomponent oxides, which would even more directly related with the early findings by Pechini. From a phenomenological point of view, no differences are expected if different metal sol are mixed and dried, provided at least one of them is introduced by a nitrate, but of course the main concern is the obtainment of a single component oxide, without phase separations. This aim is of particular importance in relationship with the preparation of technologically important materials like complex spinels, ferrites and ferroelectric materials. In establishing the fundamentals of the process, this problem has not been faced since the use of different metals in the same process would remarkably complicate the study of the involved phenomena, but it is an important step to be defined in further refinements of the process.

4. Conclusions

In this work we have introduced the sol–gel processing of metal complexes as a general route for preparing precursors for the combustion synthesis of metal oxides. The whole process, starting from the sol preparation, is simple and easily generalized, involves low combustion activation temperatures and highly exothermic reactions capable of extensive elimination of organic residuals. The morphology control of the final powder still requires an optimization of the process, and could take benefit from the possibility of growing precursor crystals, which is also useful in improving the materials utilization in the whole process. A detailed determination of the structure of the precursor species in solution and of their influence on the process, and the extension to multicomponent oxides, are open for further developments.

Acknowledgements

The authors thank Alberto Sacchetti for the XRD measurements and Maurizio Masieri for the FTIR measurements.

Appendix A. Supplementary data

Supplementary data associated with this article can be found, in the online version, at doi:10.1016/j.jeurceramsoc.2006.04.084.

References

1. (a) Merzhanov, A. G., The chemistry of self-propagating high-temperature synthesis. *J. Mater. Chem.*, 2004, **14**, 1779–1786;
(b) Moore, J. J. and Feng, H. J., Combustion synthesis of advanced materials. Part I. Reaction parameters. *Prog. Mater. Sci.*, 1995, **39**, 243–273;
(c) Moore, J. J. and Feng, H. J., Combustion synthesis of advanced materials. Part II. Classification, applications and modelling. *Prog. Mater. Sci.*, 1995, **39**, 275–316;
(d) Patil, K. C., Aruna, S. T. and Mimani, T., Combustion synthesis: an update. *Curr. Opin. Solid State Mater. Sci.*, 2002, **6**, 507–512;
(e) Wooldridge, M. S., Gas-phase combustion synthesis of particles. *Prog. Energy Combust. Sci.*, 1998, **24**, 63–97;
(f) Patil, K. C., Aruna, S. T. and Ekambaram, S., Combustion synthesis. *Curr. Opin. Solid State Mater. Sci.*, 1997, **2**, 158–165.
2. Pechini, M. P., Barium titanium citrate, barium titanate and processes for producing same. US Patent, 3,231,328, 25 January (1966).
3. Prakash, A. S., Khadar, A. M. A., Patil, K. C. and Hegde, M. S., Hexamethylenetetramine: a new fuel for solution combustion synthesis of complex metal oxides. *J. Mater. Synth. Process.*, 2002, **10**, 135–141.
4. (a) Huang, J., Zhuang, H. and Li, W., Synthesis and characterization of nanocrystalline $BaFe_{12}O_{19}$ powders by low temperature combustion. *Mater. Res. Bull.*, 2003, **38**, 149–159;
(b) Yue, Z., Guo, W., Zhou, J., Gui, Z. and Li, L., Synthesis of nanocrystalline ferrites by sol–gel combustion process: the influence of pH value of solution. *J. Magn. Magn. Mater.*, 2004, **270**, 216–223;
(c) Zhang, H., Li, L., Zhou, J., Bao, J., Yue, Z. and Gui, Z., Microstructure and properties of Co_2Z hexaferrite prepared by gel self-propagating method. *J. Mater. Sci. Mater. Electron.*, 2000, **11**, 619–622;
(d) Huang, J., Zhuang, H. and Li, W., Synthesis of barium hexaferrite powder by a modified gel combustion process. *J. Mater. Sci. Lett.*, 2003, **22**, 399–401;
(e) Li, Y., Zhao, J. and He, X., Influence of oxygen pressure on combustion synthesis of zinc ferrite powders. *Mater. Sci. Eng.*, 2004, **B106**, 196–201;
(f) Yue, Z., Zhou, J., Wang, X., Gui, Z. and Li, L., Preparation and magnetic properties of titanium-substituted LiZn ferrites via a sol-gel autocombustion process. *J. Eur. Ceram. Soc.*, 2003, **23**, 189–193;
(g) Selvan, R. K., Augustin, C. O., Berchmans, L. J. and Saraswathi, R., Combustion synthesis of $CuFe_2O_4$. *Mater. Res. Bull.*, 2003, **38**, 41–54.
5. (a) Park, H.-B., Kim, J. and Lee, C.-W. J., Synthesis of $LiMn_2O_4$ powder by auto-ignited combustion of poly(acrylic acid)-metal nitrate precursor. *Power Sources*, 2001, **92**, 124–130;
(b) Li, W., Li, J. and Guo, J., Synthesis and characterization of nanocrystalline $CoAl_2O_4$ spinel powder by low temperature combustion. *J. Eur. Ceram. Soc.*, 2003, **23**, 2289–2295;
(c) Vivekanandhan, S., Venkateswarlu, M. and Satyanarayana, N., Effect of different ethylene glycol precursors on the Pechini process for the synthesis of nano-crystalline $LiNi_{0.5}Co_{0.5}VO_4$ powders. *Mater. Chem. Phys.*, 2006, **91**, 54–59.
6. (a) Zhang, J. and Gao, L., Antimony-doped tin oxide nanocrystallites preparedby a combustion process. *Mater. Lett.*, 2004, **58**, 2730–2734;
(b) Fraigi, L. B., Lamas, D. G. and Walsöe de Reca, N. E., Comparison between two combustion routes for the synthesis of nanocrystalline SnO_2 powders. *Mater. Lett.*, 2001, **47**, 262–266;
(c) Hall, D. L., Wang, A. A., Joy, K. T., Miller, T. A. and Wooldridge, M. S., Combustion synthesis and characterization of nanocrystalline tin and tin oxide (SnO_x, $x = 0$–2) particles. *J. Am. Ceram. Soc.*, 2004, **87**, 2033–2041.
7. Zhang, J. and Gao, L., Synthesis of antimony-doped tin oxide (ATO) nanoparticles by the nitrate–citrate combustion method. *Mater. Res. Bull.*, 2004, **39**, 2249–2255.
8. (a) Mahata, T., Das, G., Mishra, R. K. and Sharma, B. P., Combustion synthesis of gadolinia doped ceria powder. *J. Alloys Compd.*, 2005, **391**, 129–135;
(b) Mokkelbost, T., Kaus, I., Grande, T. and Einarsrud, M.-A., Combustion synthesis and characterization of nanocrystalline CeO_2-based powders. *Chem. Mater.*, 2004, **16**, 5489–5494.
9. (a) Chakrabarti, N. and Maiti, H. S., Chemical synthesis of PZT powders by autocombustion of citrate-nitrate gel. *Mater. Lett.*, 1997, **30**, 169–173;
(b) Anuradha, T. V., Ranganathan, S., Mimani, T. and Patil, K. C., Combustion synthesis of nanostructured barium titanate. *Scripta Mater.*, 2001, **44**, 2237–2241;
(c) Luo, S., Tang, Z., Yao, W. and Zhang, Z., Low-temperature combustion synthesis and characterization of nanosized tetragonal barium titanate powders. *Microelectron. Eng.*, 2003, **66**, 147–152;
(d) Pasricha, R. and Ravi, V., Synthesis of $Sr_{0.5}Ba_{0.5}Nb_2O_6$ by citrate gel method. *Mater. Chem. Phys.*, 2005, **94**, 34–36.
10. (a) Deshpande, K., Mukasyan, A. and Varma, A., Direct synthesis of iron oxide nanopowders by the combustion approach: reaction mechanism and properties. *Chem. Mater.*, 2004, **16**, 4896–7904;
(b) Erri, P., Pranda, P. and Varma, A., Oxidizer-fuel interactions in aqueous combustion synthesis. 1. Iron(III) nitrate-model fuels. *Ind. Eng. Chem. Res.*, 2004, **43**, 3092–3096.

11. (a) De Sousa, V. C., Morelli, M. R., Kiminami, R. H. G. A. and Castro, M. S., Electrical properties of ZnO-based varistors prepared by combustion synthesis. *J. Mater. Sci. Mater. Electron.*, 2002, **13**, 319–325;
(b) Hwang, C.-C. and Wu, T.-Y., Combustion synthesis of nanocrystalline ZnO powders using zinc nitrate and glycine as reactants-influence of reactant composition. *J. Mater. Sci.*, 2004, **39**, 6111–6115.
12. Gallini, S., Jurado, J. R. and Colomer, M. T., Combustion synthesis of nanometric powders of $LaPO_4$ and Sr-substituted $LaPO_4$. *Chem. Mater.*, 2005, **17**, 4154–4161.
13. (a) Lian, J. S., Zhang, X. Y., Zhang, H. P., Jiang, Z. H. and Zhang, J., Synthesis of nanocrystalline NiO/doped CeO_2 compound powders through combustion of citrate/nitrate gel. *Mater. Lett.*, 2004, **58**, 1183–1188;
(b) Bayot, D. A. and Devillers, M. M., Nb-Ta, Nb-Ta-V, and Nb-Ta-Bi oxides prepared from molecular precursors based on EDTA. *Chem. Mater.*, 2004, **16**, 5401–5407;
(c) Arul Antony, S., Nagaraya, K. S., Reddy, G. L. N. and Sreedharan, O. M., A polymeric gel cum auto combustion method for the lower temperature synthesis of SrR_2O_4 (R = Y, La, Sm, Eu, Gd, Er or Yb). *Mater. Lett.*, 2001, **51**, 414–419;
(d) Santiago, E. I., Andrade, A. V. C., Paiva-Santos, C. O. and Bulhões, L. O. S., Structural and electrochemical properties of $LiCoO_2$ prepared by combustion synthesis. *Solid State Ionics*, 2003, **158**, 91–102;
(e) Murugan, B. and Ramaswamy, A. V., Nature of manganese species in $Ce_{1-x}Mn_xO_{2-\delta}$ solid solutions synthesized by the solution combustion route. *Chem. Mater.*, 2005, **17**, 3983–3993;
(f) Aruna, S. T., Ghosh, S. and Patil, K. C., Combustion synthesis and properties of $Ce_{1-x}Pr_xO_{2-\delta}$ red ceramic pigments. *Int. J. Inorg. Mater.*, 2001, **3**, 387–392;
(g) Peng, C., Liu, Y. N. and Zheng, Y. X., Nitrate–citrate combustion synthesis and properties of $Ce_{1-x}Ca_xO_{2-x}$ solid solutions. *Mater. Chem. Phys.*, 2003, **82**, 509–514.
14. Hwang, C.-C., Wu, T.-Y., Wan, J. and Tsai, J.-S., Development of a novel combustion synthesis method for synthesizing of ceramic oxide powders. *Mater. Sci. Eng. B*, 2004, **111**, 49–56.
15. (a) Yue, Z., Zhou, J., Li, L., Zhang, H. and Gui, Z., Synthesis of nanocrystalline NiCuZn ferrite powders by sol–gel auto-combustion method. *J. Magn. Magn. Mater.*, 2000, **208**, 55–60;
(b) Yue, Z., Zhou, J., Li, L., Wang, X. and Gui, Z., Effect of copper on the electromagnetic properties of Mg–Zn–Cu ferrites prepared by sol–gel auto-combustion method. *Mater. Sci. Eng. B*, 2001, **86**, 64–69;
(c) Pradeep, A. and Chandrasekaran, G., FTIR study of Ni, Cu and Zn substituted nano-particles of $MgFe_2O_4$. *Mater. Lett.*, 2006, **60**, 371–374;
(d) Guo, R. S., Wei, Q. T., Li, H. L. and Wang, F. H., Synthesis and properties of $La_{0.7}Sr_{0.3}MnO_3$ cathode by gel combustion. *Mater. Lett.*, 2006, **60**, 261–265.
16. (a) Epifani, M., Capone, S., Rella, R., Siciliano, P., Vasanelli, L., Faglia, G., Nelli, P. and Sberveglieri, G., In_2O_3 thin films obtained through a chemical complexation based sol–gel process and their application as gas sensor devices. *J. Sol–Gel Sci. Tech.*, 2003, **26**, 741–744;
(b) Epifani, M., Siciliano, P., Gurlo, A., Barman, N. and Weimar, U., Ambient pressure synthesis of corundum-type In_2O_3. *J. Am. Chem. Soc.*, 2004, **126**, 4078–4079.
17. (a) Cotton, F. A. and Wise, J. J., Assignment of the electronic absorption spectra of bis(β-ketoenolate) complexes of copper(II) and nickel(II). *Inorg. Chem.*, 1967, **6**, 917–924;
(b) Fackler, J. P., Cotton, F. A. and Barnum, D. W., Electronic spectra of β-diketone complexes. III. α-Substituted β-diketone complexes of copper(II). *Inorg. Chem.*, 1963, **2**, 97–101;
(c) Cotton, F. A. and Holm, R. H., Spectral investigations of metal complexes of β-diketones. I. Nuclear magnetic resonance and ultraviolet spectra of acetylacetonates. *J. Am. Chem. Soc.*, 1963, **80**, 5658–5663;
(d) Cotton, F. A., Electronic spectra of β-diketone complexes. IV. γ-Substituted acetylacetonates of copper(II). *Inorg. Chem.*, 1963, **2**, 102–106.
18. Colthup, N. B., Daly, L. H. and Wiberley, S. E., *Introduction to Infrared and Raman Spectroscopy* (*3rd ed.*). Academic Press, New York, 1990.
19. Nakamoto, K., *Infrared and Raman Spectra of Inorganic and Coordination Compounds. Part B: Applications in Cooordination, Organometallic, and Bioinorganic Chemistry* (*5th ed.*). Wiley, New York, NY, 1997.
20. (a) Niederberger, M., Garnweitner, G., Pinna, N. and Antonietti, M., Nonaqueous and halide-free route to crystalline $BaTiO_3$, $SrTiO_3$, and (Ba, Sr)TiO_3 nanoparticles via a mechanism involving C–C Bond formation. *J. Am. Chem. Soc.*, 2004, **126**, 9120–9126;
(b) Pinna, N., Garnweitner, G., Antonietti, M. and Niederberger, M., A General Nonaqueous Route to Binary Metal Oxide Nanocrystals Involving a C─C Bond Cleavage. *J. Am. Chem. Soc.*, 2005, **127**, 5608–5612.